Using Intracardiac Vectorcardiographic Loop for Surface ECG Synthesis

Amar Kachenoura, Fabienne Porée, Alfredo I. Hernandez, Guy Carrault

Hindawi Publishing Corporation
EURASIP Journal on Advances in Signal Processing
Volume 2008, Article ID 410630, 8 pages
doi:10.1155/2008/410630

Research Article

Using Intracardiac Vectorcardiographic Loop for Surface ECG Synthesis

A. Kachenoura,[1,2] F. Porée,[1,2] A. I. Hernández,[1,2] and G. Carrault[1,2]

[1] *Institut national de la santé et de la recherche médicale (INSERM), U642, Rennes, 35000, France*
[2] *Université de Rennes 1, Laboratoire Traitement du Signal et de l'Image (LTSI), Rennes, 35000, France*

Correspondence should be addressed to F. Porée, fabienne.poree@univ-rennes1.fr

Received 14 December 2007; Accepted 7 July 2008

Recommended by Qi Tian

Current cardiac implantable devices offer improved processing power and recording capabilities. Some of these devices already provide basic telemonitoring features that may help to reduce health care expenditure. A challenge is posed in particular for the telemonitoring of the patient's cardiac electrical activity. Indeed, only intracardiac electrograms (EGMs) are acquired by the implanted device and these signals are difficult to analyze directly by clinicians. In this paper, we propose a patient-specific method to synthesize the surface electrocardiogram (ECG) from a set of EGM signals, based on a 3D representation of the cardiac electrical activity and principal component analysis (PCA). The results, in the case of sinus rhythm, show a correlation coefficient between the real ECG and the synthesized ECG of about 0.85. Moreover, the application of the proposed method to the patients who present an abnormal heart rhythm exhibits promising results, especially for characterizing the bundle branch blocs. Finally, in order to evaluate the behavior of our procedure in some practical situations, the quality of the ECG reconstruction is studied as a function of the number of EGM electrodes provided by the CIDs.

1. INTRODUCTION

The congestive heart failure has become a major cause of morbidity and mortality. This syndrome can be treated by cardiac implantable devices (CIDs), such as cardiac resynchronization therapy pacemaker (CRT-P) and cardiac resynchronization therapy defibrillator (CRT-D). The cardiac electrical activity acquired from the CID, named electrograms (EGMs), is collected by electrodes placed on the endocardium or the epicardium. Nevertheless, they are still largely unexploited in clinical practice. Indeed, the EGM provides local information on the electric activity of a group of cardiac cells, which make their morphologies different from those observed from surface electrocardiogram (ECG) electrodes (considered as the reference signal for the analysis of the cardiac activity). Consequently, in order to perform a patient's checkup or modify the parameter settings of the CID, the acquisition of a standard surface ECG in an attended laboratory setting is required. The problem addressed in this paper concerns the possibility of estimating the standard 12-lead ECG from EGM data, so as to provide a less-expensive and less-time-consuming setup for the monitoring of the patient's cardiac electrical activity.

Several studies for standard 12-lead ECG reconstruction have been reported. They can be divided in two subcategories: those that use the linear filtering [1, 2] and those that use non linear filtering [1, 3, 4]. These works can also be classified according to the nature of the data used to synthesize surface ECG: methods described in [2–4] exploit a reduced subset of surface ECG sensors in order to estimate the standard 12-lead ECG, and the method proposed in [1] reconstructs an ECG signal from an EGM signal.

Each of these methods present some limitations. Those based on a few surface ECG leads [2–4] require the acquisition of clinical data either in an attended laboratory setting or by using an ambulatory electrocardiography device (holter monitor). Regarding the method proposed in [1], the authors suggest to reconstruct the ECG by using one EGM lead which makes the result strongly dependent on the chosen EGM. In order to overcome the limitations of the previous methods, we propose a new method to estimate a surface ECG using a set of intracardiac EGM recorded from CID electrodes. More precisely, our procedure is based on the following: (i) the extraction of a three-dimensional (3D) representation of cardiac electrical activity [5] both

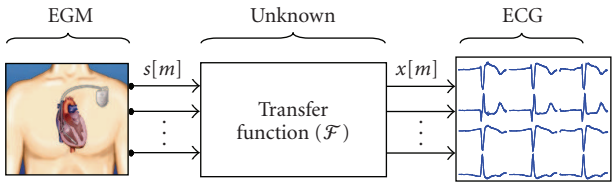

Figure 1: Problem formalization.

for surface ECG (which is called VectorCardioGram (VCG)) and for EGM (that we call VectorGram (VGM)) by using the principal component analysis (PCA) [6], and (ii) the estimation of the filter between VGM and VCG.

The paper is organized as follows: in Section 2, the standard 12-lead ECG reconstruction problem is stated and the use of both the 3D representation of cardiac electrical activity and the PCA is justified. In Section 3, the details of our procedure are provided. Section 4 gives computer results obtained in the operational context, and a conclusion is given in Section 5.

2. PROBLEM STATEMENT AND REFERENCE MATERIAL

2.1. Signal model

From the signal processing viewpoint, the problem that we propose to study can be viewed as a direct problem (Figure 1), where the outputs $\{\mathbf{x}[m]\}_{m\in\mathbb{N}}$, representing the ECG, are considered as an unspecified nonlinear function $\mathcal{F}$ of the inputs $\{\mathbf{s}[m]\}_{m\in\mathbb{N}}$, representing the EGM:

$$\mathbf{x}[m] = \mathcal{F}(\mathbf{s}[m]). \tag{1}$$

In the following, vectors are denoted by bold-faced lowercase letters, whereas bold uppercase letters denote matrices. The problem of the reconstruction of the surface ECG signal can thus be resolved in two steps, namely, the training step and the reconstruction step (Figure 2). The training step, which is performed just after the implantation, aims to identify the function $\mathcal{F}$ by using a dataset of $\mathbf{x}[m]$ (ECG) and $\mathbf{s}[m]$ (EGM) signals, simultaneously acquired in an attended laboratory setting during the implant of the CID. It is worth noting that the estimated function $\widehat{\mathcal{F}}$ is specific to each patient. The reconstruction step is devoted to the estimation of surface ECG, $\hat{\mathbf{x}}[m]$, by exploiting only the EGM, $\mathbf{s}[m]$, and the estimate, $\widehat{\mathcal{F}}$ of $\mathcal{F}$. Nevertheless, before detailing these two steps, let us give a brief description both of the 3D representation of cardiac electrical activity and PCA and justify why these two tools are used in our approach.

2.2. The 3D representation of cardiac electrical activity

The VCG is the methodological extension of ECG that provides a 3D representation of the cardiac electrical field (Figure 3). More precisely, the VCG is an orthogonal lead system that reflects the electrical activity in the three perpendicular directions X, Y, and Z. Although the 12-lead ECG is considered as the reference setup for the analysis of the cardiac activity due to the existence of a number of rules for its interpretation, the VCG contains useful information for some applications [5, 7]. Indeed, it is well known that the VCG is superior to the ECG in showing phase differences between electric events in different parts of the heart. In addition, contrary to the standard 12-lead ECG, the analysis based on VCG loops has been found to (i) better compensate the changes in the electrical axis caused by various extracardiac factors [8], such as respiration, body position, electrode positioning, and so forth, (ii) give a compact representation of the cardiac electrical activity, minimizing storage needs, and (iii) provide a solution to the time synchronization problem which arises in cardiac data. These characteristics of the 3D representation of the cardiac electrical activity seem to be useful in our case, in particular to compensate the changes in the orientation of the electrical axis estimated from EGM and ECG.

The VCG can be acquired using the traditional Frank lead system [9] or obtained by methods which establish a transformation from the standard ECG leads to the VCG domain and vice versa, such as Dower transform (DT) [10]. Since such methods do not exist in the case of EGM, we propose to extract the VGM and VCG by using PCA.

2.3. The principal component analysis

PCA, which is closely related to Karhunen-Loéve Transform (KLT) (also known as Hotelling transform), is a classical technique in statistical data analysis, features extraction, and data compression. The purpose of PCA is to derive a relatively small number of uncorrelated linear combinations (principal components) of a set of random zero-mean variables while retaining as much of the information from the original variables as possible [6]. Typically, the PCA of vector $\mathbf{x}[m] = [x[m]_1, \ldots, x[m]_N]^\mathsf{T}$ consists in looking for an $N \times P$ orthonormal linear transform $\mathbf{W}$ (P smaller or equal to N), such that

$$\mathbf{z}[m] = \mathbf{W}^\mathsf{T}\mathbf{x}[m], \tag{2}$$

where the components of the vector $\mathbf{z}[m] = [z[m]_1, \ldots, z[m]_P]^\mathsf{T}$ are mutually uncorrelated. Sometimes, we need the columns of the matrix $\mathbf{W}$; if we denote w_{np} ($1 \le n \le N$ and $1 \le p \le P$) the elements of $\mathbf{W}$, the model of (2) can also be written as

$$z_p[m] = \sum_{n=1}^{N} w_{np} x_n[m] = \mathbf{w}_p^\mathsf{T}\mathbf{x}[m]. \tag{3}$$

The first principal component, $z_1[m]$, of the vector $\mathbf{x}[m]$ is obtained by looking for the weight vector $\mathbf{w}_1$ that maximizes, under constraint that $\|\mathbf{w}_1\| = 1$, the variance of $z_1[m]$. Thus the PCA criterion can be written as follows:

$$\begin{aligned}\Psi(\mathbf{w}_1, z_1[m]) &= \mathsf{E}[z_1[m]^2] = \mathsf{E}\left[\left(\mathbf{w}_1^\mathsf{T}\mathbf{x}[m]\right)^2\right] \\ &= \mathbf{w}_1^\mathsf{T}\mathsf{E}[\mathbf{x}[m]\mathbf{x}[m]^\mathsf{T}]\mathbf{w}_1 = \mathbf{w}_1^\mathsf{T}\mathbf{R}_\mathbf{x}\mathbf{w}_1,\end{aligned} \tag{4}$$

where $\mathsf{E}[\cdot]$ denotes the mathematical expectation and $\mathbf{R}_\mathbf{x}$ the $N \times N$ covariance matrix of $\mathbf{x}$. From (4), PCA can be converted to the eigenvalue problem of the covariance matrix $\mathbf{R}_\mathbf{x}$.

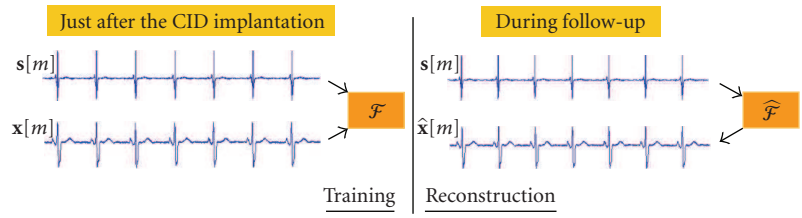

Figure 2: A two-step proposed procedure.

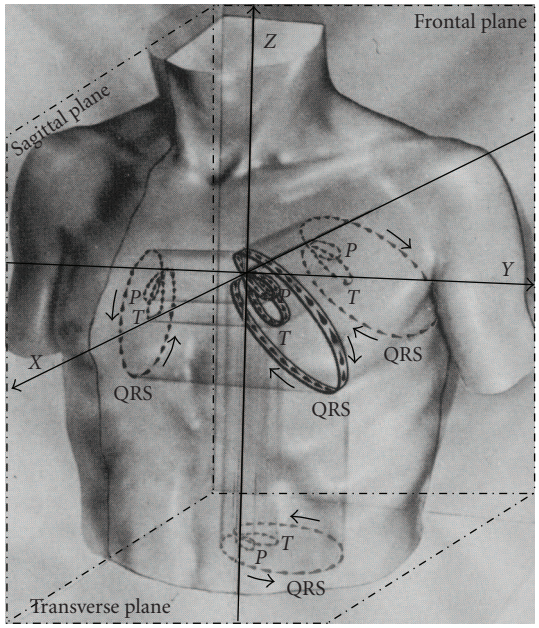

Figure 3: The VCG loop and its projection onto the three orthogonal planes [5].

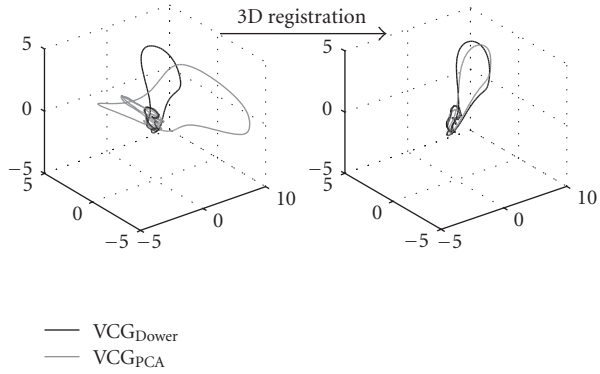

Figure 4: Comparison between the synthesized VCG loops: black line is obtained by Dower and gray line is obtained using PCA.

In fact, if we denote $[\mathbf{e}_1 \dots \mathbf{e}_P]^\mathsf{T}$ the eigenvectors of $\mathbf{R_x}$ corresponding to the eigenvalues $(\lambda_1, \dots, \lambda_P)$, where $\lambda_1 \geq \cdots \geq \lambda_P$, the solution maximizing the PCA criterion (4) is obtained by $\mathbf{w}_1 = \mathbf{e}_1$ and the first principal component of $\mathbf{x}[m]$ is $z_1[m] = \mathbf{e}_1^\mathsf{T}\mathbf{x}[m]$. The criterion described in (4) is then generalized to P principal components and the pth $(1 < p \leq P)$ principal component $z_p[m]$ is obtained by maximizing the PCA criterion $\Psi(\mathbf{w}_p, z_p[m])$ under the constraint that $z_p[m]$ is uncorrelated with all the previously found principal components. For example, in the case of the second component $z_2[m]$, we have the condition that $\mathbf{w}_2^\mathsf{T}\mathbf{R_x}\mathbf{w}_1 = \lambda_1\mathbf{w}_2^\mathsf{T}\mathbf{e}_1 = 0$. Then, it is straightforward to show that the second principal component of $\mathbf{x}$ is given by $z_2[m] = \mathbf{e}_2^\mathsf{T}\mathbf{x}[m]$. Likewise, recursively the Pth principal component is $z_P[m] = \mathbf{e}_P^\mathsf{T}\mathbf{x}[m]$. Figure 4 shows that the synthesized VCG loops obtained using PCA and the DT are nearly identical, after the application of a 3D registration step [8]. This result strengthen us in our conviction that the use of PCA is an appropriate tool for our study.

3. A TWO-STEP PROCESSING APPROACH

The aim of this section is to provide more information (see Figure 5) about the two steps of our procedure, namely, the training step and the reconstruction step.

3.1. *Training step*

This step (Figure 5(a)) can be decomposed into three substeps: the identification of the orthonormal linear transform $\mathbf{W}$, between the ECG ($\mathbf{x}[m]$) and the VCG ($\mathbf{z}_{\mathrm{VCG}}[m]$), the 3D registration of the VGM loops ($\mathbf{z}_{\mathrm{VGM}}[m]$), and the estimation of the filter $\mathbf{h}[m]$ between the VCG and the registered VGM loops.

Identification of $\mathbf{W}$

Let us assume that $\mathbf{x}[m] = [x_1[m], \dots, x_N[m]]^\mathsf{T}_{m=1,\dots,M}$ (where $N \geq 3$ is the number of ECG leads and M is the number of records) represents the ECG of L successive heartbeats. The orthonormal linear transform $\mathbf{W}$ is estimated by applying the PCA on $\mathbf{x}[m]$ so that the following result holds:

$$\mathbf{z}_{\mathrm{VCG}}[m] = \mathbf{W}^\mathsf{T}\mathbf{x}[m]. \tag{5}$$

It is worth noting that once the $N \times P$ matrix $\mathbf{W}$ is identified, only the components of interest are considered. In our case, we just take into account the three principal components, corresponding to the three largest eigenvalues of the covariance matrix $\mathbf{R_x}$, which provides us an $N \times 3$ matrix $\mathbf{W}$.

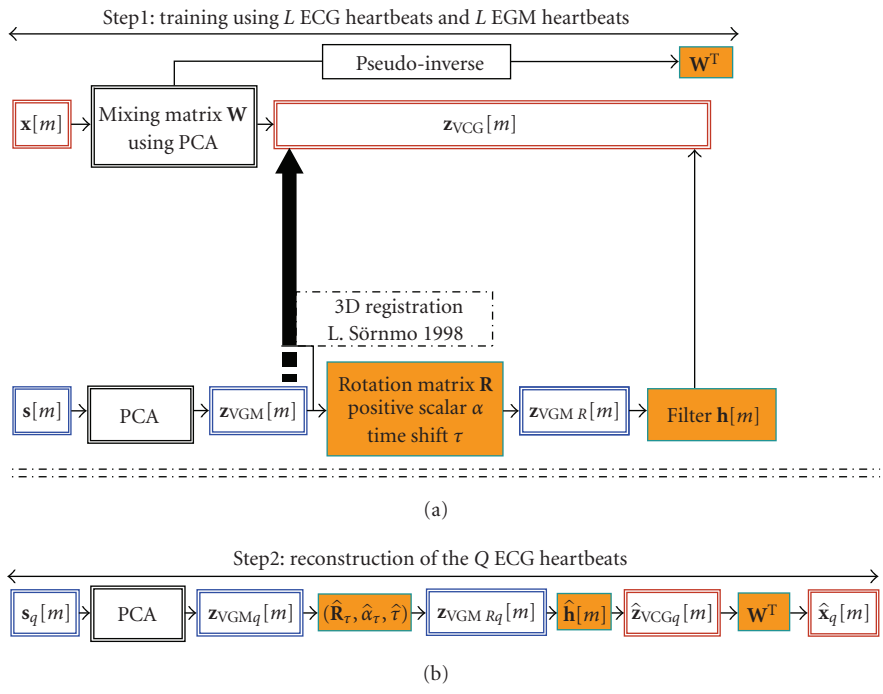

Figure 5: Detailed representation of our procedure: (a) training step, (b) reconstruction step.

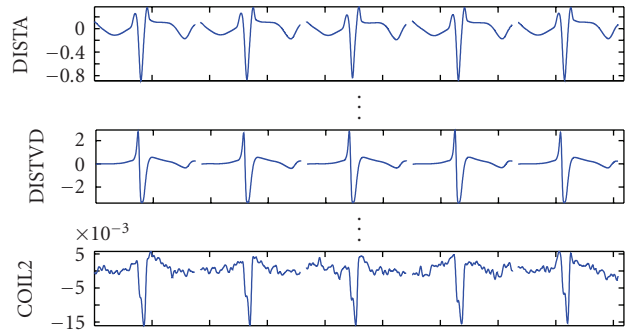

Figure 6: Example of a patient with sinus rhythm: EGM channels.

The VGM 3D registration

In order to improve the precision of some automatic ECG analysis algorithms, Sörnmo proposed in [8] a preprocessing method to compensate for heartbeat morphology variations during an ECG/VCG recording. This method, based on four steps, is applied here to the registration of VGM loops. The four steps can be summarized as follows.

(i) *Translation:* a baseline-filtering technique is applied to eliminate the slow baseline wander caused by the electrode impedance changes.

(ii) *Scaling:* contraction/dilatation of the loop is modeled by the positive scalar α.

(iii) *Rotation:* positional changes of the heart are modeled by rotating VGM loop with the 3×3 orthonormal matrix $\mathbf{R}$.

(iv) *Time synchronisation:* an integer time shift τ is introduced in the signal model by the shift matrix $\mathbf{J}_\tau$ in order to improve the time synchronization of the loops.

Let us assume that the VCG loop is considered in our case as a reference loop. As for ECG, let $\mathbf{s}[m] = [s_1[m], \ldots, s_K[m]]^T$ (where $K \geq 3$ is the number of EGM leads) be the EGM of L successive heartbeats. The VGM, $\mathbf{z}_{\mathrm{VGM}}[m]$, is firstly derived by applying the PCA on $\mathbf{s}[m]$, where we just take into account the three largest eigenvalues of the covariance matrix $\mathbf{R}_{\mathbf{s}}$. Then, both $\mathbf{z}_{\mathrm{VCG}}[m]$ and $\mathbf{z}_{\mathrm{VGM}}[m]$ are segmented into L nonoverlapping blocks of equal length T, $\mathbf{z}_{\mathrm{VCG}\ell}[m]_{\ell=1,\ldots,L}$ and $\mathbf{z}_{\mathrm{VGM}\ell}[m]_{\ell=1,\ldots,L}$, respectively. Now let us consider the expectations of $\mathbf{z}_{\mathrm{VCG}\ell}[m]_{\ell=1,\ldots,L}$ and $\mathbf{z}_{\mathrm{VGM}\ell}[m]_{\ell=1,\ldots,L}$ estimated by averaging over the number of heartbeats L using the following sample formula [11]:

$$\begin{aligned} \bar{\mathbf{z}}_{\mathrm{VCG}}[m] &= \frac{1}{L}\sum_{\ell=1}^{L} \mathbf{z}_{\mathrm{VCG}\ell}[m], \\ \bar{\mathbf{z}}_{\mathrm{VGM}}[m] &= \frac{1}{L}\sum_{\ell=1}^{L} \mathbf{z}_{\mathrm{VGM}\ell}[m]. \end{aligned} \tag{6}$$

In order to include the time synchronisation step, it is necessary to subtract 2Δ samples to the reference loop $\bar{\mathbf{z}}_{\mathrm{VCG}}[m]$, which provides us a new $3 \times T - 2\Delta$ reference loop $\tilde{\bar{\mathbf{z}}}_{\mathrm{VCG}}[m]$. The estimation of $\mathbf{R}$, α, and τ is based on a model in which the VGM loop $\bar{\mathbf{z}}_{\mathrm{VGM}}[m]$ is related to the reference loop $\tilde{\bar{\mathbf{z}}}_{\mathrm{VCG}}[m]$ as follows:

$$\tilde{\bar{\mathbf{z}}}_{\mathrm{VCG}}[m] = \alpha \mathbf{R} \bar{\mathbf{z}}_{\mathrm{VGM}}[m] \mathbf{J}_\tau, \tag{7}$$

where $\tau = -\Delta, \ldots, \Delta$ and $\mathbf{J}_\tau = [\ \mathbf{0}_{\Delta-\tau}\ \mathbf{I}\ \ \mathbf{0}_{\Delta+\tau}\ ]^T$. The dimensions of the left and right zero matrices are equal to $\Delta - \tau \times T - 2\Delta$ and $\Delta + \tau \times T - 2\Delta$, respectively.

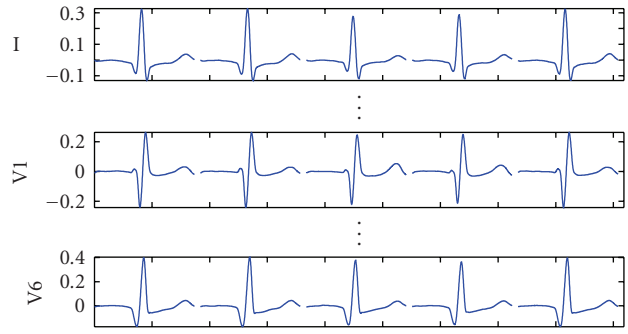

Figure 7: Example of a patient with sinus rhythm: real ECG channels.

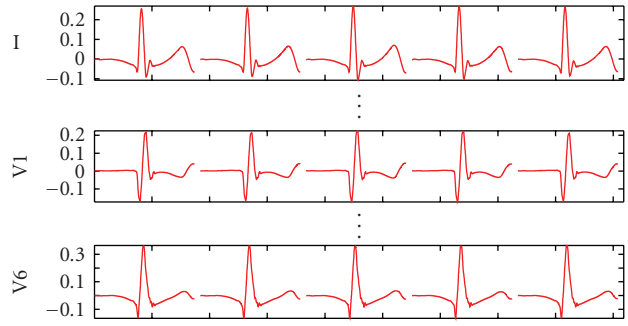

Figure 8: Example of a patient with sinus rhythm: reconstructed ECG channels (ECGR).

It is easy to show that the estimation of $\mathbf{R}$, α, and τ can be reduced to the following minimization problem [8]:

$$\xi^2_{\min} = \min_{\alpha,\mathbf{R},\tau} ||\widetilde{\bar{\mathbf{z}}}_{\mathrm{VCG}}[m] - \alpha\mathbf{R}\bar{\mathbf{z}}_{\mathrm{VGM}}[m]\mathbf{J}_\tau||^2_F, \tag{8}$$

where $\|\cdot\|_F$ denotes the Frobenius norm. The minimization of the previous equation is performed by first finding the estimates $\hat{\alpha}$ and $\hat{\mathbf{R}}$ by fixing τ. The optimal estimates α, $\mathbf{R}$, and τ are then determined by evaluating the error ξ^2 for different values of τ. Then, the estimate of $\mathbf{R}$ is given by

$$\hat{\mathbf{R}}_\tau = \mathbf{U}\mathbf{V}^{\mathsf{T}}, \tag{9}$$

where the columns of $\mathbf{U}$ and $\mathbf{V}$ are the left and right eigenvectors of the matrix $\widetilde{\bar{\mathbf{z}}}_{\mathrm{VCG}}[m]\mathbf{J}_\tau^{\mathsf{T}}\bar{\mathbf{z}}_{\mathrm{VGM}}[m]^{\mathsf{T}}$. The estimate of α is determined as follows:

$$\hat{\alpha}_\tau = \frac{\mathtt{tr}\left(\mathbf{J}_\tau^T\bar{\mathbf{z}}_{\mathrm{VGM}}[m]\hat{\mathbf{R}}_\tau^T\widetilde{\bar{\mathbf{z}}}_{\mathrm{VCG}}[m]\right)}{\mathtt{tr}\left(\mathbf{J}_\tau^T\bar{\mathbf{z}}_{\mathrm{VGM}}\widehat{[m]}^{\mathsf{T}}\bar{\mathbf{z}}_{\mathrm{VGM}}[m]^{\mathsf{T}}\mathbf{J}_\tau\right)}. \tag{10}$$

The parameter τ is estimated by

$$\hat{\tau} = \arg\min_\tau = ||\widetilde{\bar{\mathbf{z}}}_{\mathrm{VCG}}[m] - \hat{\alpha}_\tau\hat{\mathbf{R}}_\tau\bar{\mathbf{z}}_{\mathrm{VGM}}[m]\mathbf{J}_\tau||^2_F. \tag{11}$$

Finally, the registered VGM loop $\bar{\mathbf{z}}_{\mathrm{VGMR}}[m]$ is derived from (7) using the following equation:

$$\bar{\mathbf{z}}_{\mathrm{VGMR}}[m] = \hat{\alpha}_{\hat{\tau}}\hat{\mathbf{R}}_{\hat{\tau}}\bar{\mathbf{z}}_{\mathrm{VGM}}[m]\mathbf{J}_{\hat{\tau}}. \tag{12}$$

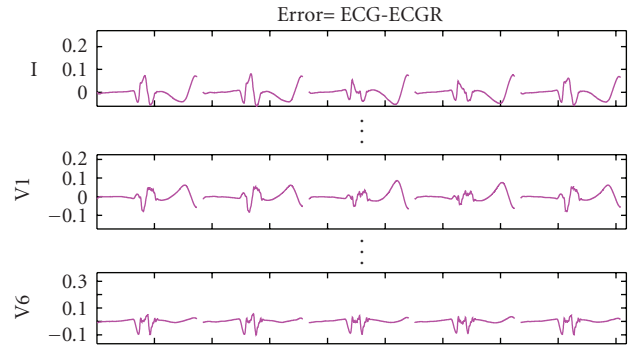

Figure 9: Example of a patient with sinus rhythm: reconstruction errors.

Estimation of the filter $\mathbf{h}[m]$

In order to estimate $\mathbf{h}[m]$, we must estimate three different transfert functions $h_1[m]$, $h_2[m]$, and $h_3[m]$ between each row of the output vector $\widetilde{\bar{\mathbf{z}}}_{\mathrm{VCG}}[m]$ and each row of the input vector $\bar{\mathbf{z}}_{\mathrm{VGMR}}[m]$. For the sake of readability, let us consider the estimation of $h_1[m]$, which is characterized by the input-output relationship:

$$\widetilde{\bar{z}}_{\mathrm{VCG}_1}[m] = (\bar{z}_{\mathrm{VGMR}_1} * h_1)[m] = \sum_{i=0}^{Lh-1} h_1[i]\bar{z}_{\mathrm{VGMR}_1}[m-i], \tag{13}$$

where $*$ denotes the convolution operator. In vector notation, it reads

$$\widetilde{\bar{z}}_{\mathrm{VCG}_1}[m] = \mathbf{h}_1\bar{\mathbf{z}}_{\mathrm{VGMR}_1}[m], \tag{14}$$

where the Lh-dimensional parameter vector $\mathbf{h}_1 \overset{\mathrm{def}}{=} [h_1(0), \ldots, h_1(Lh-1)]^{\mathsf{T}}$ is the impulse response of a linear time invariant (LTI) filter, and $\bar{\mathbf{z}}_{\mathrm{VGMR}_1}[m] \overset{\mathrm{def}}{=} [\bar{z}_{\mathrm{VGMR}_1}[m], \ldots, \bar{z}_{\mathrm{VGMR}_1}[m-Lh+1]]^{\mathsf{T}}$. An estimate, $\hat{\mathbf{h}}_1$, of $\mathbf{h}_1$, can thus be derived from the general Wiener-Hopf equation [12] which relates the optimal LTI filter to the covariance matrix of the output $\mathbf{R}_{\widetilde{\bar{z}}}$ and to the intercorrelation between the output and the input $\mathbf{R}_{\widetilde{\bar{z}}\bar{z}}$, such that

$$\hat{\mathbf{h}}_1 = \mathbf{R}_{\widetilde{\bar{z}}}^{-1}\mathbf{R}_{\widetilde{\bar{z}}\bar{z}}. \tag{15}$$

The same result can be directly derived for $\mathbf{h}_2$ and $\mathbf{h}_3$.

3.2. Reconstruction step

This step (Figure 5(b)) is devoted to the estimation of surface ECG by exploiting the EGM and different parameters identified in the training step. To do so, we suppose that we only observe the EGM of Q successive heartbeats, denoted by $\mathbf{s}[m] = [s_1[m], \ldots, s_K[m]]^{\mathsf{T}}_{m=1,\ldots,M'}$ (where M' is the number of records of the EGM used in the reconstruction step). Then, $\mathbf{s}[m]$ is segmented into Q nonoverlapping blocks of equal length T, $\mathbf{s}_q[m]_{q=1,\ldots,Q}$, and the PCA is applied on each block, which provides us Q VGM blocks $\mathbf{z}_{\mathrm{VGM}\,q}[m]_{q=1,\ldots,Q}$

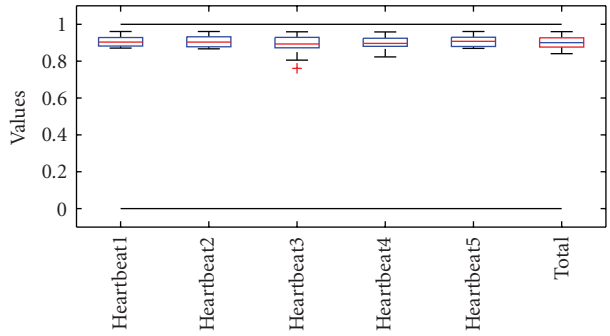

Figure 10: Boxplots of the correlation coefficients, obtained for a patient with sinus rhythm, between ECG and ECGR for each heartbeat and for the 12 ECG channels.

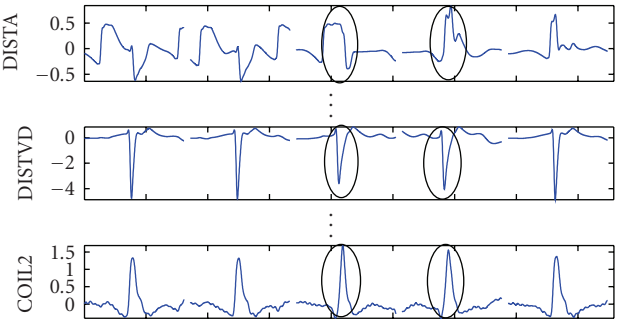

Figure 11: Example of a patient with cardiac arrhythmia: EGM channels.

(as for the training step, only the three first principal components are taken into account). Finally, the Q heartbeats surface ECG are estimated one by one as follows:

$$\hat{\mathbf{x}}_q[m] = \left(\hat{\alpha}_{\hat{\tau}}\hat{\mathbf{R}}_{\hat{\tau}}\mathbf{z}_{\mathrm{VGMR}\,q}\mathbf{J}_{\hat{\tau}} * \hat{\mathbf{h}}\right)[m]\mathbf{W}^{\mathsf{T}}, \quad \forall q \in \{1,\ldots,Q\}. \tag{16}$$

4. RESULTS

4.1. Database description

A dataset issued from 12 patients (P1 to P12) is used for evaluating the proposed method. The ECG and EGM are simultaneously recorded with a GE Cardiolab station during the implant of CIDs with a sampling rate equal to 1000 Hz. Each record of the database is composed of 12 surface ECG channels, namely, I, II, III, AVR, AVL, AVF, V1, to V6, and 4 to 7 EGM electrodes depending on CID type. More precisely, three different CID types have been used to acquire our signals: a triple chamber defibrillator for patients P1 to P6, a triple chamber pacemaker for P7 to P9, and a dual chamber pacemaker for patients P10 to P12. Table 1 summarizes the EGM leads acquired from each patient on the database, where VD, VG, A, DIST, PROX, COIL1, and COIL2 denote the right ventricular, left ventricular, right atrium, distal tip electrodes, proximal ring electrodes, the coil for ventricular defibrillation, and the coil for supraventricular defibrillation, respectively. We also observed that 10 patients of the database

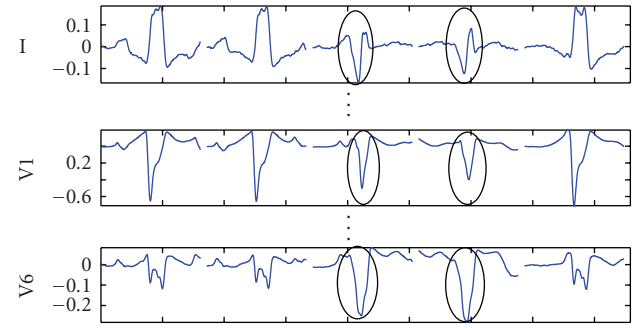

Figure 12: Example of a patient with cardiac arrhythmia: real ECG channels.

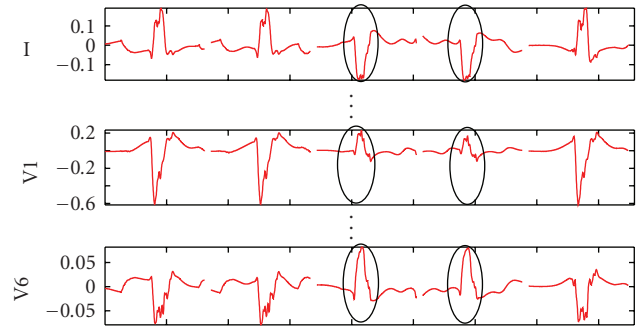

Figure 13: Example of a patient with cardiac arrhythmia: reconstructed ECG channels.

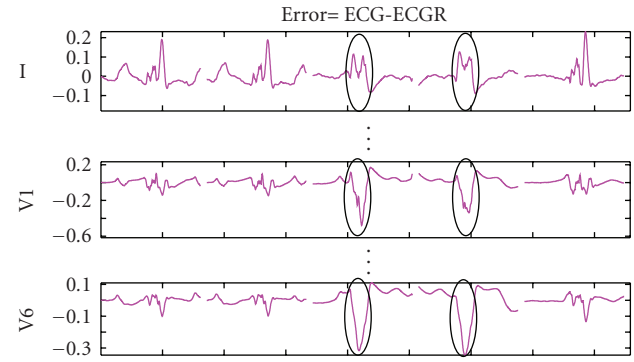

Figure 14: Example of a patient with cardiac arrhythmia: reconstruction errors.

present an ECG with a sinus rhythm, whereas cardiac arrhythmia (premature ventricular complexes) are detected for two patients (P2 and P7).

Each patient's data is segmented into two blocks. The first block contains $L = 10$ heartbeats of concurrent ECG and EGM signals, and is used in the training step in order to estimate the transfer function between EGM and ECG (see Section 3.1). The second block contains $Q = 5$ heartbeats and is devoted to the reconstruction step (see Section 3.2).

4.2. Performance evaluation

The objective of this section is twofold: (i) to show the behavior of our method both for the patients with sinus

Table 1: For each patient of the database, the number of available EGM electrodes varies from 4 to 7: P2 and P7 (bold case) are the patients with cardiac arrhythmias.

	P1	**P2**	P3	P4	P5	P6	**P7**	P8	P9	P10	P11	P12
DISTA	+	+	+	+	+	+	+	+	+	+	+	+
PROXA	+	+	+	+	+	+	+	+	+	+	+	+
DISTVD	+	+	+	+	+	+	+	+	+	+	+	+
PROXVD	+	+	+	+	+	+	+	+	+	+	+	+
DISTVG	+	+	+	+	+	+	+	+	+			
COIL1	+	+	+	+	+	+						
COIL2	+	+	+	+	+	+						

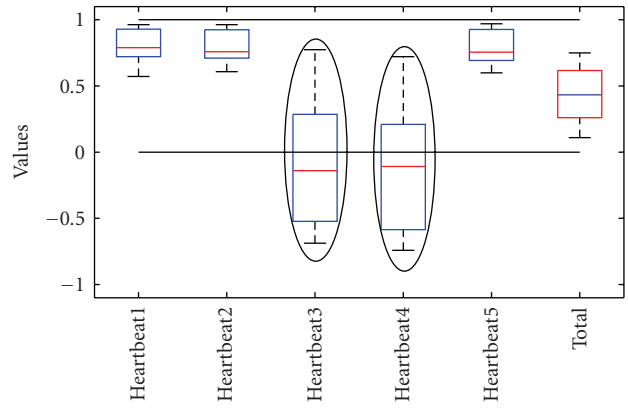

Figure 15: Boxplots of the correlation coefficients, obtained for a patient with cardiac arrhythmia, between ECG and ECGR for each heartbeat and for the 12 ECG channels.

rhythm and for the patients with cardiac arrhythmia, and (ii) to evaluate the quality of the 12-lead ECG reconstruction as a function of the number and location of EGM electrodes exploited by our procedure. This last point is investigated in this paper in order to evaluate the behavior of our procedure in some practical situations where the CIDs provide only three or two implantable electrodes.

Figures 6, 7, and 8 show an example of EGM channels recorded from the CID, the real surface ECG and the synthesized ECG (ECGR), respectively, for a patient with sinus rhythm (P3). Clearly, all the heartbeats are well estimated (Figure 8). Indeed, Figure 9 shows, for each heartbeat and each ECG channel, that the reconstructions errors are practically insignificant, especially for the QRS complexes. This result is also confirmed by the correlation coefficient between ECG and ECGR (Figure 10), estimated for the 12 ECG channels, which is about 0.90 for the five distinct heartbeats.

Figures 11 and 12 illustrate an example of EGM channels and real ECG (Patient P2), where two similar premature ventricular contractions (PVCs) are observed (the third and fourth heartbeat, which are surrounded by a circle on Figures 11 to 15). As depicted in Figure 13, sinus beats are well reconstructed (Figure 15 shows that their correlation coefficients are about 0.8). Regarding the heartbeats with PVC, our method seems to provide less reliable estimates. Indeed, the reconstruction errors for the third and fourth beats are significant (Figure 14) and their correlation coefficients are about −0.2 (see Figure 15). However, the behavior of our procedure is promising since the reconstructed pathological morphologies are very different from sinus beats and since the morphology of the reconstructed beats remains the same for a given original beat morphology. Moreover, the QRS width is preserved, even if the morphology of the reconstructed beat is not always well reproduced. Thus, even if our procedure is not able to exactly reproduce some beat morphologies, it can be used to detect abnormal ECG rhythms. In addition, the preservation of the QRS width can be particularly useful to characterize bundle branch blocs from reconstructed beats.

In order to evaluate the quality of the 12-lead ECG reconstruction as a function of the number of EGM electrodes, our procedure is applied to all the database by exploiting (i) all the available EGM electrodes, (ii) three EGM electrodes, namely, DISTA, DISTVD, and DISTVG (case of triple chamber pacemakers), and (iii) two EGM electrodes, DISTA and DISTVD (which are the electrodes commonly available on dual chamber pacemakers). Note that, in the latter case, the VCG and the VGM are firstly derived by applying the PCA on the ECG and the EGM, respectively, where we just take into account the two largest eigenvalues of the covariance matrices of ECG and EGM. Then, an extended version of our approach to the 2D is used to the 12-lead ECG reconstruction (the 2D version of our procedure can be easily realized from Section 3 and is thus omitted in this paper).

Figure 16 displays the obtained results both for each patient (Figure 16(a)) and for each ECG channel (Figure 16(b)). We can observe that the ECG reconstruction for patient P2 and P7 (Figure 16(a)) is less effective in comparison to the other patients. This result is due to the fact that P2 and P7 present cardiac arrhythmia. Figure 16(b) show that the quality of reconstruction is independent of a particular ECG channel. It is very interesting to note that both for each patient and for each ECG channel, the performance obtained using three EGM (dark gray bars) are quasi-identical than those obtained by all available EGM (black bars), whereas our procedure seems to be less effective when only two electrodes are exploited (light gray bars). This comes essentially from the fact that, in the cases where three or more EGM electrodes are used, the information provided by both sides of the heart are exploited, while when disposing of only two electrodes, we only exploit the activity of the right side of the heart.

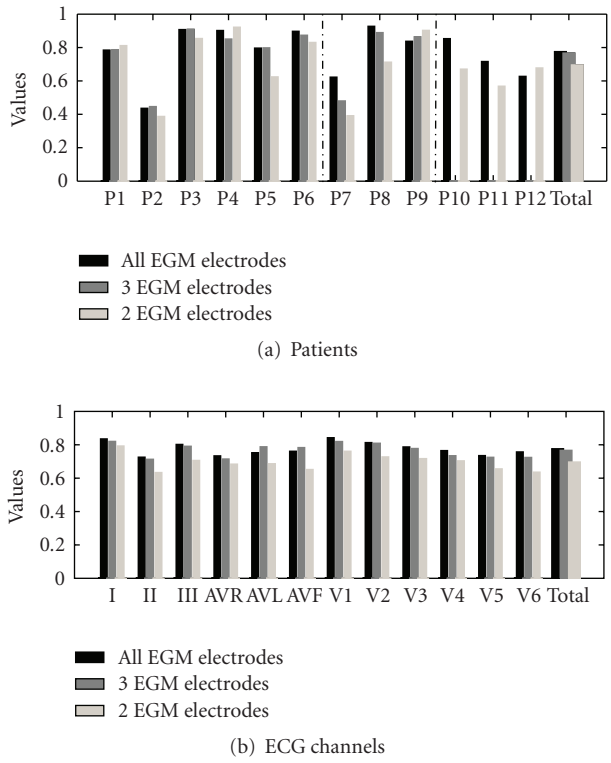

Figure 16: The correlation coefficient between ECG and ECGR using all EGM channels (black bars), using three EGM channels (dark gray bar) and using two EGM channel (light gray bar): (a) for each patient and (b) for each channel.

5. CONCLUSION

The CRT-P and CRT-D are examples of devices that have been successfully used for the treatment of the clinical syndrome of congestive heart failure. However, in order to perform a patient's checkup or modify the parameter setting of the CID, the acquisition of a standard surface ECG in an attended laboratory is required. Up to now, the intracardiac EGM are collected by the implanted devices. However, these signals are difficult to analyze directly by clinicians because they only provide local information on the electric activity of a group of cardiac cells. To overcome this limitation, we propose in our study a patient-specific method to synthesize a surface ECG by exploiting a set of EGM signals. This method is based on the 3D representation of cardiac electrical activity, both for surface ECG (VCG) and intracardiac EGM (VGM), which is extracted by using PCA.

The obtained results show a very good behavior of our procedure in the case of patients with sinus rhythm (correlation coefficient between the real ECG and the reconstructed ECG is about 0.85). Regarding the patients who present abnormal heart beats, our procedure seems to provide promising results. Indeed, preliminary results show that the reconstructed pathological morphologies are very different from sinus beats and the morphology of the reconstructed beats remains the same for a given original beat morphology. Thus, our procedure can be viewed as a detector of abnormal ECG beats. In addition, the QRS width of the abnormal beat seems to be preserved, which makes our procedure particularly useful to characterize bundles branch blocs from the reconstructed ECG. Another interesting results show that the performance of our procedure by using only three EGM electrodes or a high number of EGM (seven and five EGM electrodes in our case) is quasi-identical. Moreover, even if our procedure seems to be less effective when only two electrodes are exploited, the quality of the reconstruction is still satisfactory (correlation coefficient about 0.70). These last results are very interesting in the practical cases where most of CIDs provide only three or two implantable electrodes.

ACKNOWLEDGMENT

This work has been supported by the ANR Contract no. 991-388-ZVANG.

REFERENCES

[1] M. Gentil, F. Porée, A. I. Hernández, and G. Carrault, "Surface electrocardiogram reconstruction from cardiac prothesis electrograms," in *Proceedings of the 3rd European Medical and Biological Engineering Conference (EMBEC '05)*, p. 2028F1-6, Prague, Czech Republic, November 2005.

[2] S. P. Nelwan, J. A. Kors, S. H. Meij, J. H. van Bemmel, and M. L. Simoons, "Reconstruction of the 12-lead electrocardiogram from reduced lead sets," *Journal of Electrocardiology*, vol. 37, no. 1, pp. 11–18, 2004.

[3] H. Atoui, J. Fayn, and P. Rubel, "A neural network approach for patient-specific 12-lead ECG synthesis in patient monitoring environments," in *Proceedings of the Computers in Cardiology Conference*, vol. 31, pp. 161–164, Chicago, Ill, USA, September 2004.

[4] C. Vásquez, A. Hernández, F. Mora, G. Carrault, and G. Passariello, "A trial activity enhancement by Wiener filtering using an artificial neural network," *IEEE Transactions on Biomedical Engineering*, vol. 48, no. 8, pp. 940–944, 2001.

[5] T. Winsor, *Primer of Vectorcardiography*, Lea & Febiger, Philadelphia, Pa, USA, 1972.

[6] K. I. Diamantaras and S. Y. Kung, *Principal Component Neural Networks: Theory and Applications*, Wiley-Interscience, New York, NY, USA, 1996.

[7] L. Sörnmo and P. Laguna, *Bioelectrical Signal Processing in Cardiac and Neurological Applications*, Elsevier, Academic Press, New York, NY, USA, 2005.

[8] L. Sörnmo, "Vectorcardiographic loop alignment and morphologic beat-to-beat variability," *IEEE Transactions on Biomedical Engineering*, vol. 45, no. 12, pp. 1401–1413, 1998.

[9] E. Frank, "An accurate, clinically practical system for spatial vectorcardiography," *Circulation*, vol. 13, pp. 737–749, 1956.

[10] G. E. Dower, H. B. Machado, and J. A. Osborne, "On deriving the electrocardiogram from vectorcardiographic leads," *Clinical Cardiology*, vol. 3, no. 2, pp. 87–95, 1980.

[11] P. McCullagh, *Tensor Methods in Statistics*, Monographs on Statistics and Applied Probability, Chapman & Hall/CRC, London, UK, 1987.

[12] B. Picinbono, *Random Signal and Systems*, Prentice-Hall, Upper Saddle River, NJ, USA, 1993.